Interfacial Assembly and Jamming of Polyelectrolyte Surfactants: A Simple Route To Print Liquids in Low-Viscosity Solution

Ruiyan Xu, Tan Liu, Huilou Sun, Beibei Wang, Shaowei Shi,* and Thomas P. Russell*

ABSTRACT: Nanoparticle surfactants (NPSs) assembled at the oil−water interface can significantly lower the interfacial tension and be used to structure liquids. However, to realize the three- dimensional printing of one liquid in another, high-viscosity liquids, for example, silicone oil, have been generally used. Here, we present a simple, low-cost approach to print water in low- viscosity toluene by using a new type of polyelectrolyte surfactant, sodium carboxymethyl cellulose surfactant (CMCS), that forms and assembles at the oil−water interface. The interfacial activity of CMCSs can be enhanced by tuning parameters, such as pH and concentration, and the incorporation of a rigid ligand affords excellent mechanical strength to the resultant assemblies. With CMCS jammed at the interface, liquids can be easily printed or molded to the desired shapes, with biocompatible walls that can be used to encapsulate and adsorb active materials. This study opens a new pathway to generate complex, all-liquid devices with a myriad of potential applications in biology, catalysis, and chemical separation.

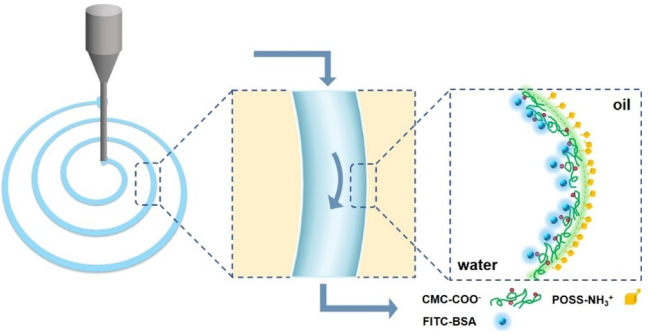

KEYWORDS: *polyelectrolyte surfactant, structured liquids, jamming, 3D printing, transmission*

INTRODUCTION

The liquid−liquid interface affords an ideal platform for the organized assembly of nanomaterials in a constrained environment and for the generation of hierarchical structures where the inherent properties of nanomaterials can be integrated into the structure.[1,2] Colloidal assemblies from the mesoscale (e.g., colloidosomes) to the macroscale (e.g., 2D films and foams) have been reported, spurring great academic interest and having technological value.[3−7] Recently, using nanoparticle surfactants (NPSs), a new concept of materials, termed structured liquids, was proposed by Cui et al.[8] This system consists of nanoparticles (NPs) and polymer/oligomer surfactants, bearing complementary functional groups, that are initially dispersed in two immiscible phases, for example, water and oil. NPSs are formed in situ and assemble at the interface and can jam to lock-in nonequilibrium shapes of liquids.

With NPSs, liquids can be sculpted using external fields, such as electric and shear.[9,10] Forth et al. adapted the NPS system to generate three-dimensional (3D) printed aqueous structures in a high-viscosity (60 000 cSt at 25 °C) silicone oil.[11] To produce well-defined aqueous threads in oil, the assembly rate of NPSs must be high enough in comparison to the timescale of the thread breakup because of the Plateau− Rayleigh (PR) instabilities. This timescale is given by $\tau = \alpha\mu r/\gamma$, where μ is the viscosity of the external phase, r is the thread diameter, γ is the oil−water interfacial tension, and α is a

numerical factor of order 10 that depends on the viscosity ratio between the internal and external phases.[12−14] This final timescale makes 3D printing of liquids in a low-viscosity oil rather challenging.[2,15] It is desirable, therefore, to find NPS systems with highly interfacial activity, for example, cellulose nanocrystal surfactants.[16−18]

Polyelectrolytes are polymers that carry numerous positively or negatively charged groups, hence they can interact through electrostatic interactions. Under most conditions, when mixed, the oppositely charged polyelectrolytes interact, forming a coacervate, a macroscopic phase separation of the electrostatic complex and excess solvent plus small ions.[19] By the formation of an interfacial coacervate, polyelectrolyte microcapsules have been successfully generated in oil−water systems and aqueous two-phase systems (ATPSs).[20−25] Very recently, by using 3D printing and immiscible solutions of poly(ethylene glycol) and dextran, all-aqueous 3D printed tubular flow systems have been produced.[26] However, unlike ATPSs with extremely low interfacial tension, in oil−water systems, the interfacial tension is usually large, and the less plastic nature of coacervates may

lead to the deformation or collapse of the structured assemblies.

Here, we present a simple, low-cost strategy to print liquids in low-viscosity solutions using the interfacial coassembly of a widely used polyelectrolyte, sodium carboxymethyl cellulose (CMC),[27,28] and amine-functionalized polyhedral oligomeric silsesquioxane (POSS-NH_2) across the toluene−water inter- face (Scheme 1 and Figure 1a). As the smallest NP of

Scheme 1. Chemical Structure of CMC, POSS-NH_2, and PS- NH_2

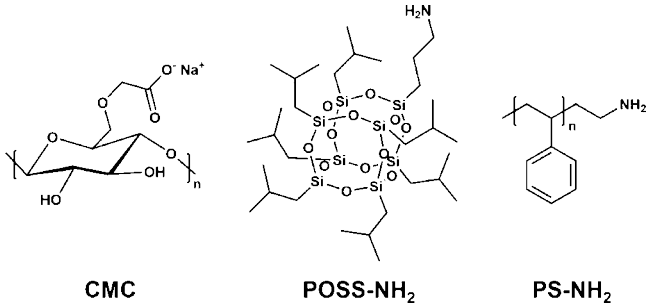

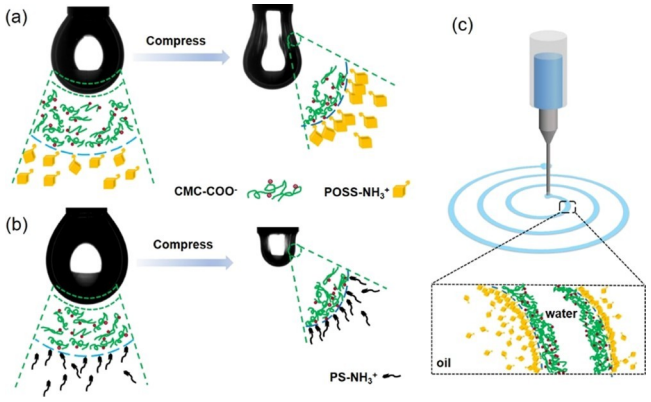

Figure 1. Schematic representation of the assembling and jamming of CMCSs at the toluene−water interface. (a) With rigid POSS-NH_2 dissolved in toluene; (b) with soft PS-NH_2 dissolved in toluene; and (c) printing of water in oil with CMCS assemblies at the toluene−water interface.

molecular silica, POSS molecules have a precisely defined structure with a rigid, cubic inorganic silica-cage core with side chains that endow the interfacial assemblies with mechanical strength.[29,30] As a control experiment, amine-terminated polystyrene (PS-NH_2) is used as a “soft” ligand to interact with CMC at the interface (Scheme 1 and Figure 1b). We find that by tuning parameters, such as pH and concentration of CMC/ligand, CMC surfactants (CMCSs) can be formed and assemble rapidly at the oil−water interface, and when jammed, they offer a robust assembly that is responsive. With “rigid” POSS-NH_2 dissolved in the oil phase, liquids can be easily printed or molded with excellent structural stability and can be used to encapsulate active materials because of the biocompatible CMC walls, showing great potential in the fabrication of all-liquid microfluidic devices (Figure 1c).[31]

RESULTS AND DISCUSSION

The kinetics of the CMCS formation and assembly at the oil− water interface was measured by tracking the dynamic interfacial tension (γ) using pendant drop tensiometry. As a

type of anionic polyelectrolyte, CMC is rich in carboxylic acid groups. By adjusting the pH of an aqueous CMC solution, the degree of protonation of the carboxylic acid groups and the charge density can be controlled (Figure 2a). We first investigated the interfacial activity of pristine CMC by varying the pH of the aqueous solution from 7.0 to 3.0. As shown in Figure 2b-c, CMC is not interfacially active in a neutral pH environment (pH = 7.0) with an equilibrium interfacial tension of ~35 mN/m, which is close to that of the pure water− toluene system (~36 mN/m). By decreasing the pH from 7.0 to 4.0 and then to 3.0, the equilibrium interfacial tension reduces gradually from 35 to 32 and then to 28 mN/m, indicating an increased interfacial activity of CMC. At a lower pH, the protonation degree of the carboxylic acid groups increases, leading to the enhanced hydrophobicity of CMC and hence the spontaneous segregation of CMC at the oil−water interface. However, when reducing the volume of the droplet to decrease the interfacial area and compress the interfacial assembly, the binding energy is not sufficient to withstand the compressive force, and CMCs are rejected from the interface, showing a liquid-like behavior (Video S1).

POSS-NH_2 and PS-NH_2 behave as surfactants and can assemble at the oil−water interface, reducing the interfacial tension (Figure S2). With POSS-NH_2 or PS-NH_2 dissolved in the toluene phase with CMC dissolved in the aqueous phase, the interfacial activity of CMC can be greatly enhanced by forming CMCS at the oil−water interface. Here, we set the molar concentration of the amine group of POSS-NH_2 or PS- NH_2 as 0.10 mM and the molar concentration of CMC as 4.0 × 10^{-4} mM. As shown in Figure 3a−c, by decreasing the pH from 6.0 to 3.0, the equilibrium interfacial tensions of both systems decrease gradually, indicating the formation and assembly of CMCS at the interface and its pH-dependent characteristics, which is dictated by the ammonium-carboxylate ion pairing. By decreasing the pH, more amine groups can be protonated, giving rise to stronger electrostatic interactions between CMCs and ligands. The coverage (C) of the interface with the CMCSs on the droplet is estimated from the ratio S_J/ S_F, where S_J and S_F are surface areas for the jammed and free (initial) states, respectively.[32] We note that in comparison to PS-NH_2, at the same pH, the equilibrium surface coverage of CMCS using POSS-NH_2 as the ligand is always higher (Figure 3d and Video S2), indicating that the mechanical strength of the interface is enhanced by introducing rigid POSS-NH_2, making the assemblies more solid-like. By increasing the concentration of either CMC or the ligand, the interfacial activity of CMCSs can be further increased (Figures S3 and S4).

In the following experiments, the pH value of the aqueous phase is fixed at 3.0 to ensure that the interfacial activity and the surface coverage of CMCs are high, which is beneficial for structuring liquids, for example, suppressing the PR instabilities of liquids during printing.

To quantify the mechanical properties of interfacial assemblies, storage and loss dilatational moduli, $E'(\omega)$ and $E''(\omega)$, of the interfacial assemblies were investigated by oscillatory pendant drop tensiometry/rheometry at low concentrations of CMC and ligands.[33] As shown in Figure 4a, the elastic modulus $E'(\omega)$ is higher than the loss modulus $E''(\omega)$ over the entire frequency range used for the measurements (0.01−1 Hz), which demonstrates that the interfacial assembly is elastic. With rigid POSS-NH_2 dissolved in toluene, the $E'(\omega)$ of the interfacial CMC/POSS-NH_2 assembly is significantly higher than that of the CMC/PS-

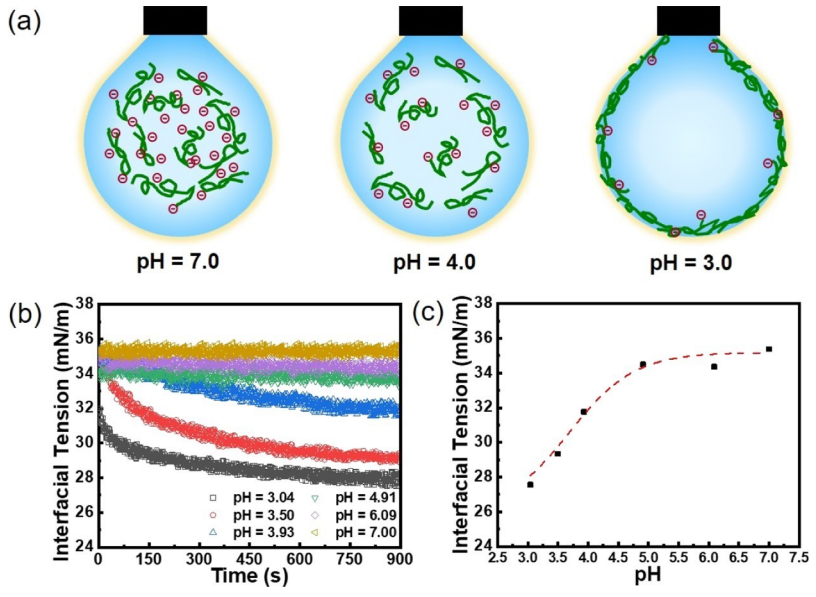

Figure 2. (a) Schematic representation of the interfacial activity of CMC with different pHs; (b) time evolution of interfacial tension; and (c) equilibrium interfacial tension between CMC aqueous solution and pure toluene with different pHs. [CMC] = 4.0×10^{-4} mM.

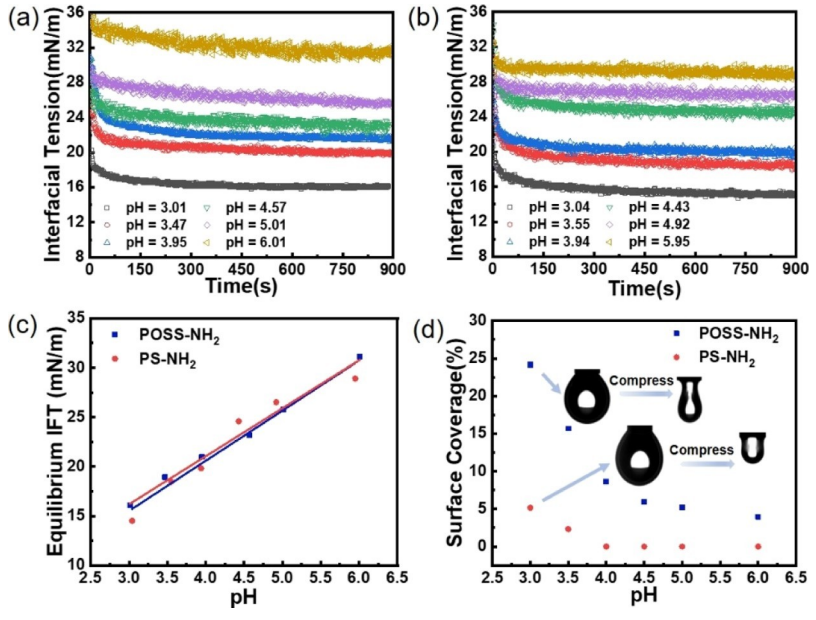

Figure 3. Time evolution of interfacial tension between CMC aqueous solution and toluene dissolving (a) POSS-NH_2 and (b) PS-NH_2 with different pHs; (c) equilibrium interfacial tension with different pHs; and (d) surface coverage of CMCS as a function of pH in the equilibrium state. [CMC] = 4.0×10^{-4} mM, [POSS-NH_2] = 0.10 mM, [PS-NH_2] = 0.10 mM.

NH_2 assembly, although the concentration of POSS-NH_2 ([POSS-NH_2] = 0.10 mM) in toluene is much lower than that of PS-NH_2 ([PS-NH_2] = 0.30 mM). The more solid-like nature of CMC/POSS-NH_2 assemblies can be confirmed by forcing a needle into an existing droplet. As shown in Figure 4b, with CMC/PS-NH_2 assemblies at the interface, after squeezing the droplet with the needle, no breakage of the droplet is observed and the interfacial assemblies show an elastic behavior (Video S3). However, with CMC/POSS-NH_2 assemblies at the interface, after squeezing the droplet with the needle, the interfacial assemblies show a solid-like behavior, and an obvious deformation of the droplet is observed, indicating that the droplet can be easily structured, owing to the easier interfacial jamming of CMCSs when using POSS-

NH_2 (Video S4). In a pendent drop mode, when the droplet is fully withdrawn into the needle and then reinjected to the initial volume, the interfacial CMC/POSS-NH_2 assemblies contort into unusual shapes but ultimately returned to the initial droplet shape. This extraction−reinjection process can be repeated multiple times with no evidence of cracking, further indicating the robust nature of the CMC/POSS-NH_2 assemblies (Figure 4c and Video S5). For the CMC/PS-NH_2 assemblies, the extraction−reinjection process is completely different, where the wrinkles are observed only at very large compression ratios and an elongation of the droplet is observed during extraction (Figure S5 and Video S6).

When using soft PS-NH_2 as the ligand, upon compressing the interface, CMCSs can reorganize, leading to a responsive-

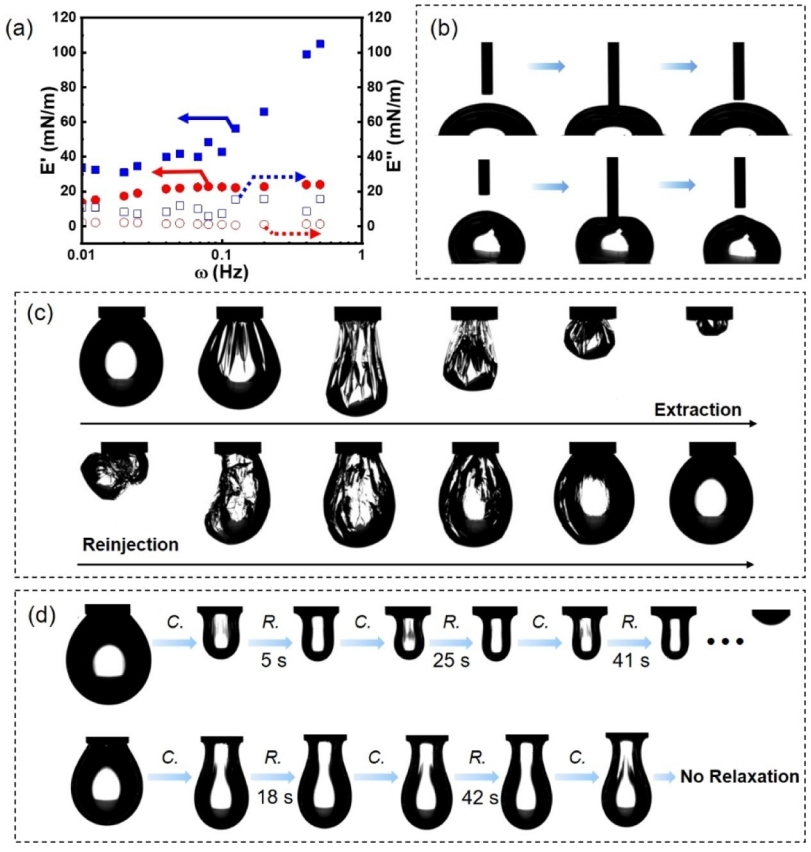

Figure 4. (a) Storage and loss dilatational moduli, $E'(\omega)$and $E''(\omega)$, of CMC/PS-NH_2 assemblies (red) and CMC/POSS-NH_2 assemblies (blue), [CMC] = 4.0 × 10^{-4} mM, [PS-NH_2] = 0.30 mM, [POSS-NH_2] = 0.10 mM; (b) sequence of snapshots showing the process of contact, compression, and separation of the needle and droplet. The bottom droplets were formed by injecting 4.0 × 10^{-3} mM CMC aqueous solution into 1.0 mM PS-NH_2 (up) or POSS-NH_2 (bottom) toluene solution; (c) snapshots of droplet's morphology evolution in an extraction−reinjection process, [CMC] = 4.0 × 10^{-3} mM, [POSS-NH_2] = 1.0 mM; (d) snapshots of droplet's morphology upon a repeated compression−relaxation experiment, [CMC] = 4.0 × 10^{-4} mM, [PS-NH_2] = 0.10 mM, [POSS-NH_2] = 0.10 mM.

ness to an applied external field, such as compression or gravity, and thus, the droplet elongates. With rigid POSS-NH_2 as the ligand, the reorganization of CMCSs is significantly inhibited because of the enhanced mechanical strength of the assembly. A compression−relaxation experiment was performed (Figure 4d) to confirm this, where the volume of the droplet is first reduced until the wrinkles are observed, and then the volume is kept constant to see whether the assemblies relax. In the case of CMC/PS-NH_2 assemblies, the wrinkles rapidly relax, indicating that upon compression, CMCSs reorganize rapidly, changing the interfacial assemblies from a solid-like jammed state to an elastomer-like unjammed state. If we further compress the droplet, wrinkling is again observed; however, the relaxation occurs over a longer time. This compression−relaxation process can be repeated several times until the density of CMCSs at the interface is exceptionally high so that the relaxation is impeded or takes an exceptional long time. For CMC/POSS-NH_2 assemblies, wrinkles can be obtained at very small compressions. The relaxation of the interfacial assemblies can only be found after the first two compressions and the relaxation time is longer than that of CMC/PS-NH_2 assemblies. Subsequently, the wrinkles do not relax, indicating that the CMCSs are jammed and reorganiza- tion of CMCSs does not occur.

Before producing tubules by 3D printing, the effect of CMCSs on PR instabilities of water jets was investigated using the tensiometer in a flush mode by forcing aqueous CMC

solutions ([CMC] = 4.0 × 10^{-3} mM) into toluene solutions of PS-NH_2 or POSS-NH_2 through a narrow capillary. As shown in Figure 5a, at low concentration of PS-NH_2 in toluene ([PS-NH_2] = 1.3 mM), no continuous tubules were obtained, and the aqueous phase rapidly broke up into droplets. Tubular structures could only be obtained at a very high PS-NH_2 concentration ([PS-NH_2] = 13 mM) (Figure S6). With POSS- NH_2 dissolved in toluene ([POSS-NH_2] = 2.3 mM), continuous tubular structures were easily produced (Figure 5b and Video S7). No breakup was observed in jetting and the tubules formed that rested at the bottom of the cell did not coalesce and were stable for more than 1 month. From the surface coverage measurements, with a low POSS-NH_2 concentration of 0.60 mM, full coverage (100%) can be achieved within 10 s (Figure S7). Using a 3D printer, threads of aqueous CMC solutions can be printed in a toluene solution of POSS-NH_2 with diameters from 500 μm to 2.0 mm by tuning the diameter of the needle, print head rate, and flow rate, which can be used for the dye transmission (Figures 5c,d and S8 and Videos S8 and S9). The liquid tubules are pH- responsive because of the pH-dependent characteristics of CMCSs. With the injection of NaOH solution into the printed liquids, the binding energy between CMC and POSS-NH_2 can be significantly weakened, leading to a damage of the tubule liquids (Figure S9 and Video S10). By taking advantage of the biocompatible CMC walls with negative charges, positively charged fluorescein isothiocyanate bovine serum albumin

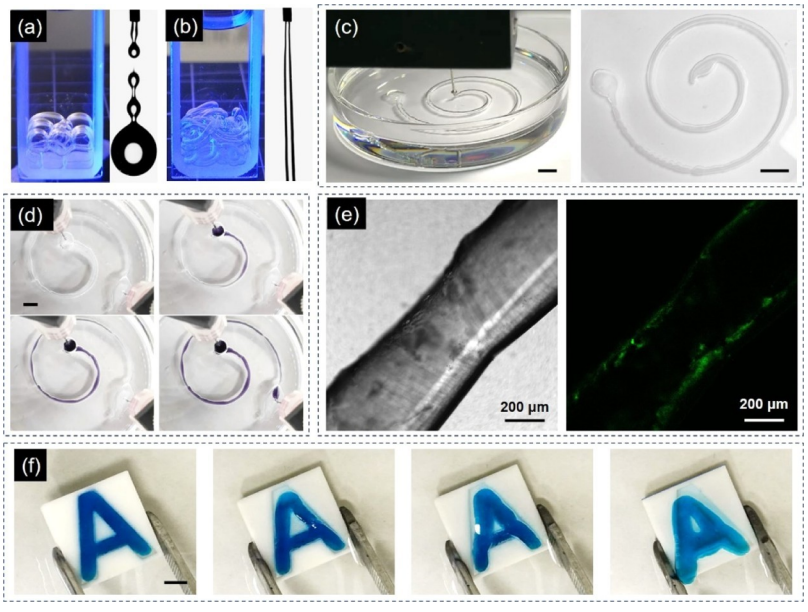

Figure 5. High-speed photography of an aqueous CMC solution falling in toluene solution containing (a) PS-NH_2 or (b) POSS-NH_2 and the formed droplets or tubule liquid in the bottom of the cell, [CMC] = 4.0×10^{-3} mM, [PS-NH_2] = 1.3 mM, [POSS-NH_2] = 2.3 mM, flow rate = 2.0 mL/min; (c) 3D printing of CMCS-stabilized aqueous threads in toluene (left) and the produced aqueous spiral (right), injection rate = 2.0 mL/min; (d) screenshots of the transmission of a dye solution, [Congo red] = 0.07 mM, transmission rate = 5 mL/h; (e) optical (left) and confocal fluorescence (right) microscopy image of tubule liquid after the adsorption of FITC-BSA in the wall; (f) dyed liquid letter "A" molded by the interfacial jamming of CMCs using POSS-NH_2 dissolved in CCl_4, [CMC] = 4.0×10^{-3} mM, [POSS-NH_2] = 2.3 mM, [Nile blue] = 0.07 mM, scale bar: 5 mm.

(FITC-BSA) can be successfully adsorbed to the inner wall of the tubule (Figure 5e). Finally, owing to the high interfacial activity of CMCSs and the robust nature of the assemblies, all-liquid objects can also be produced by a molding strategy, which retains the shape and details of the mold with high fidelity (Figure 5f and Video S11).[17]

CONCLUSIONS

In summary, we have presented a simple approach to print liquids in low-viscosity liquid media by using a polyelectrolyte surfactant, CMCS. All the materials are of low cost and can be easily obtained. The interfacial activity of CMCS can be effectively tuned by changing the pH and concentration, and the mechanical strength can be enhanced by introducing a rigid ligand, POSS-NH_2, which is beneficial for the construction of structured liquids. Taken together, these results offer great application potentials in fields such as biphasic reactions, drug delivery, and all-liquid separation systems.

ACKNOWLEDGMENTS

This work was supported by the National Natural Science
Foundation of China (51903011) and Beijing Natural Science Foundation (2194083). T.P.R. was supported by the U.S. Department of Energy, Office of Science, Office of Basic Energy Sciences, Materials Sciences and Engineering Division under Contract no. DE-AC02-05-CH11231 within the Adaptive Interfacial Assemblies Towards Structuring Liquids program (KCTR16).

REFERENCES

(1) Shi, S.; Russell, T. P. Nanoparticle Assembly at Liquid-Liquid
Interfaces: From the Nanoscale to Mesoscale. *Adv. Mater.* 2018, *30*, 1800714.

(2) Forth, J.; Kim, P. Y.; Xie, G.; Liu, X.; Helms, B. A.; Russell, T. P. Building Reconfigurable Devices Using Complex Liquid-Fluid Interfaces. *Adv. Mater.* 2019, *31*, 1806370.

(3) Binks, B. P.; Lumsdon, S. O. Influence of Particle Wettability on the Type and Stability of Surfactant-Free Emulsions. *Langmuir* 2000, *16*, 8622−8631.

(4) Aveyard, R.; Binks, B. P.; Clint, J. H. Emulsions Stabilised Solely by Colloidal Particles. *Adv. Colloid Interface Sci.* 2003, *100−102*, 503− 546.

(5) Böker, A.; He, J.; Emrick, T.; Russell, T. P. Self-Assembly of Nanoparticles at Interfaces. *Soft Matter* 2007, *3*, 1231−1248.

(6) Niu, Z.; He, J.; Russell, T. P.; Wang, Q. Synthesis of Nano/ Microstructures at Fluid Interfaces. *Angew. Chem., Int. Ed.* 2010, *49*, 10052−10066.

(7) Hu, L.; Chen, M.; Fang, X.; Wu, L. Oil-Water Interfacial Self-
Assembly: A Novel Strategy for Nanofilm and Nanodevice Fabrication. *Chem. Soc. Rev.* 2012, *41*, 1350−1362.

(8) Cui, M.; Emrick, T.; Russell, T. P. Stabilizing Liquid Drops in
Nonequilibrium Shapes by the Interfacial Jamming of Nanoparticles.
Science 2013, *342*, 460−463.

(9) Huang, C.; Forth, J.; Wang, W.; Hong, K.; Smith, G. S.; Helms,
B. A.; Russell, T. P. Bicontinuous Structured Liquids with Sub- micrometre Domains Using Nanoparticle Surfactants. *Nat. Commun.* 2017, *12*, 1060−1063.

(10) Liu, X.; Kent, N.; Ceballos, A.; Streubel, R.; Jiang, Y.; Chai, Y.;
Kim, P. Y.; Forth, J.; Hellman, F.; Shi, S.; Wang, D.; Helms, B. A.; Ashby, P. D.; Fischer, P.; Russell, T. P. Reconfigurable Ferromagnetic Liquid Droplets. *Science* 2019, *365*, 264−267.

(11) Forth, J.; Liu, X.; Hasnain, J.; Toor, A.; Miszta, K.; Shi, S.; Geissler, P. L.; Emrick, T.; Helms, B. A.; Russell, T. P. Reconfigurable Printed Liquids. *Adv. Mater.* 2018, *30*, 1707603.
(12) Tomotika, S. On the instability of a cylindrical thread of a viscous liquid surrounded by another viscous fluid. *Proc. R. Soc. London, Ser. A* 1935, *150*, 322−337.
(13) Powers, T. R.; Zhang, D.; Goldstein, R. E.; Stone, H. A.
Propagation of a Topological Transition: The Rayleigh Instability.
Phys. Fluids 1998, *10*, 1052−1057.
(14) Homma, S.; Koga, J.; Matsumoto, S.; Song, M.; Tryggvason, G.
Breakup Mode of an Axisymmetric Liquid Jet Injected into Another Immiscible Liquid. *Chem. Eng. Sci.* 2006, *61*, 3986−3996.
(15) Toor, A.; Helms, B. A.; Russell, T. P. Effect of Nanoparticle
Surfactants on the Breakup of Free-Falling Water Jets during Continuous Processing of Reconfigurable Structured Liquid Droplets. *Nano Lett.* 2017, *17*, 3119−3125.
(16) Liu, X.; Shi, S.; Li, Y.; Forth, J.; Wang, D.; Russell, T. P. Liquid
Tubule Formation and Stabilization Using Cellulose Nanocrystal Surfactants. *Angew. Chem., Int. Ed.* 2017, *56*, 12594−12598.
(17) Li, Y.; Liu, X.; Zhang, Z.; Zhao, S.; Tian, G.; Zheng, J.; Wang,
D.; Shi, S.; Russell, T. P. Adaptive Structured Pickering Emulsions and Porous Materials Based on Cellulose Nanocrystal Surfactants. *Angew. Chem., Int. Ed.* 2018, *57*, 13560−13564.
(18) Shi, S.; Liu, X.; Li, Y.; Wu, X.; Wang, D.; Forth, J.; Russell, T. P.
Liquid Letters. *Adv. Mater.* 2018, *30*, 1705800.
(19) Overbeek, J. T. G.; Voorn, M. J. Phase Separation in Polyelectrolyte Solutions. *J. Cell. Physiol.* 1957, *49*, 7−26.
(20) Monteillet, H.; Hagemans, F.; Sprakel, J. Charge-Driven Co- Assembly of Polyelectrolytes across Oil−Water Interfaces. *Soft Matter* 2013, *9*, 11270−11275.
(21) Kaufman, G.; Boltyanskiy, R.; Nejati, S.; Thiam, A. R.;
Loewenberg, M.; Dufresne, E. R.; Osuji, C. O. Single-Step Microfluidic Fabrication of Soft Monodisperse Polyelectrolyte Microcapsules by Interfacial Complexation. *Lab Chip* 2014, *14*,
3494−3497.
(22) Kim, M.; Yeo, S. J.; Highley, C. B.; Burdick, J. A.; Yoo, P. J.;
Doh, J.; Lee, D. One-Step Generation of Multifunctional Polyelec- trolyte Microcapsules via Nanoscale Interfacial Complexation in Emulsion (NICE). *ACS Nano* 2015, *9*, 8269−8278.
(23) Hann, S. D.; Niepa, T. H. R.; Stebe, K. J.; Lee, D. One-Step
Generation of Cell-Encapsulating Compartments via Polyelectrolyte Complexation in an Aqueous Two Phase System. *ACS Appl. Mater. Interfaces* 2016, *8*, 25603−25611.
(24) Ma, Q.; Song, Y.; Kim, J. W.; Choi, H. S.; Shum, H. C. Affinity
Partitioning-Induced Self-Assembly in Aqueous Two-Phase Systems: Templating for Polyelectrolyte Microcapsules. *ACS Macro Lett.* 2016, *5*, 666−670.
(25) Zhang, L.; Cai, L.-H.; Lienemann, P. S.; Rossow, T.; Polenz, I.;
Vallmajo-Martin, Q.; Ehrbar, M.; Na, H.; Mooney, D. J.; Weitz, D. A. One-Step Microfluidic Fabrication of Polyelectrolyte Microcapsules in Aqueous Conditions for Protein Release. *Angew. Chem., Int. Ed.* 2016,
55, 13470−13474.
(26) Xie, G.; Forth, J.; Chai, Y.; Ashby, P. D.; Helms, B. A.; Russell,
T. P. Compartmentalized, All-Aqueous Flow-Through-Coordinated Reaction Systems. *Chem* 2019, *5*, 2678−2690.
(27) Qiu, X.; Hu, S. “Smart” Materials Based on Cellulose: A Review
of the Preparations, Properties, and Applications. *Materials* 2013, *6*, 738−781.
(28) Hubbe, M. A. Review of the Mechanistic Roles of Nano-
cellulose, Cellulosic Fibers, and Hydrophilic Cellulose Derivatives in Cellulose-Based Absorbents. *Cellulose-Based Superabsorbent Hydrogels*; Springer International Publishing, 2018; pp 123−153.
(29) Hou, H.; Li, J.; Li, X.; Forth, J.; Yin, J.; Jiang, X.; Helms, B. A.;
Russell, T. P. Interfacial Activity of Amine-Functionalized Polyhedral Oligomeric Silsesquioxanes (POSS): A Simple Strategy to Structure Liquids. *Angew. Chem., Int. Ed.* 2019, *58*, 10142−10147.
(30) Shi, S.; Qian, B.; Wu, X.; Sun, H.; Wang, H.; Zhang, H.-B.; Yu,
Z.-Z.; Russell, T. P. Self-Assembly of MXene-Surfactants at Liquid-

(31) Feng, W.; Chai, Y.; Forth, J.; Ashby, P. D.; Russell, T. P.; Helms, B. A. Harnessing liquid-in-liquid printing and micropatterned substrates to fabricate 3-dimensional all-liquid fluidic devices. *Nat. Commun.* 2019, *10*, 1095.

(32) Sun, Z.; Feng, T.; Russell, T. P. Assembly of graphene oxide at water/oil interfaces: tessellated nanotiles. *Langmuir* 2013, *29*, 13407− 13413.

(33) Huang, C.; Cui, M.; Sun, Z.; Liu, F.; Helms, B. A.; Russell, T. P. Self-Regulated Nanoparticle Assembly at Liquid/Liquid Interfaces: A Route to Adaptive Structuring of Liquids. *Langmuir* 2017, *33*, 7994− 8001.